Anti-tumor effect of the mammalian target of rapamycin inhibitor everolimus in oral squamous cell carcinoma

Tomofumi Naruse, Souichi Yanamoto, Shin-ichi Yamada, Satoshi Rokutanda, Akiko Kawakita, Goro Kawasaki, Masahiro Umeda

Department of Clinical Oral Oncology, Unit of Translational Medicines, Nagasaki University Graduate School of Biomedical Sciences, 1-7-1 Sakamoto, Nagasaki 852-8588, Japan

Key words: oral cancer, mTOR, everolimus, hypoxia

Running title: Anti-tumor effect of the mammalian target of rapamycin inhibitor everolimus in oral squamous cell carcinoma

Corresponding author. Tel.: + 81 95 819 7698 fax: + 81 95 819 7700.

E-mail: naruse12@nagasaki-u.ac.jp (T. Naruse)

Abstract

Objectives: The mammalian target of rapamycin (mTOR) has recently emerged as a promising target for therapeutic anti-cancer interventions in several human tumors. In present study, we investigated the expression of mTOR, and subsequently examined its relationship with clinicopathological factors and the anti-tumor effect of everolimus (also known as RAD001) in oral squamous cell carcinoma (OSCC).

Material and Methods: The expression of phosphorylated mTOR (p-mTOR) was immunohistochemically evaluated in specimens obtained from 70 OSCC patients who underwent radical surgery. The relationships between the expression of p-mTOR and clinicopathological factors and survival were determined. We also investigated the effect of everolimus on the OSCC cell lines, SAS, HSC-2, HSC-3, HSC-4, OSC-20, SCC25 and Ca9-22 by the MTT assay. We further evaluated whether mTOR contributed to cell functions by blocking its activity with everolimus, and confirmed the direct target by the Matrigel invasion assay, wound healing assay and Western blotting.

Results: p-mTOR was overexpressed in 37 tumors (52.8%), and correlated with the T classification, N classification, and survival rate ($P<0.05$). The treatment with everolimus significantly inhibited cell growth, and significantly reduced the expression of p-mTOR, downstream signaling proteins, and hypoxic related proteins as well as invasion and migration potentials ($P<0.05$).

Conclusions: The results of the present study suggest that everolimus may represent an attractive approach for the future treatment of OSCC.

Introduction

Oral squamous cell carcinoma (OSCC) is the most common malignant tumor of the head and neck region, and its incidence has recently been increasing [1]. The current management and treatment of OSCC involves multimodal approaches comprising surgery, chemotherapy, and radiotherapy [2]. Despite recent advances in early detection, diagnosis, and treatment, the 5-year survival rate for patients with OSCC has remained at 50% for the past 30 years [3]. Because of the high prevalence and mortality rates of oral cancers, new treatment strategies are required.

The mammalian target of rapamycin (mTOR) is a 289-KDa serine/threonine kinase belonging to the phosphoinositide 3-kinase (PI3K)-related kinase family that regulates cell growth, proliferation, and progression of the cell cycle [4]. mTOR is activated by the phosphorylation of Ser2448 through the PI3K/AKT signaling pathway, and completes these functions by activating p70 ribosomal S6 kinase ($p70^{S6K}$) and phosphorylating the eukaryotic initiation factor 4E binding protein 1 (4E-BP1) [4, 5, 7]. Moreover, this pathway promotes the translation of hypoxia-inducible factor-1α (HIF-1α) mRNA coding for pro-oncogenic proteins and regulates its expression and activity [6, 7]. HIF-1α is one of the main regulators of cellular adaptaion to hypoxia and is known to be stabilized and translocated to the nucleus under hypoxic conditions, and induces the expression of the vascular endothelial growth factor (VEGF) and other tumor growth factors [6-9]. Furthermore, several studies have indicated that the expression of HIF-1α is associated with resistance to chemotherapy and radiotherapy [10-12]. Therefore, a more detailed examination of this pathway should be performed in OSCC.

Activated mTOR has been associated with poor prognosis in various cancers including OSCC [13-16], and some researchers have indicated the effectiveness of mTOR

inhibitors in various cancers [16-20]. However, the anti-tumor effect of the mTOR inhibitor in OSCC under hypoxic conditions remains unclear. Everolimus (RAD001) is an orally bioavailable derivative of rapamycin and initially forms a complex with 12kDa FK506-binding protein (FKBP-12). This complex then binds to the FKBP-12-Rapamycin Binding (FRB) domain of mTOR, and inhibits the function of mTOR [21]. Everolimus has been approved for the treatment of metastatic renal cell carcinoma [22], progressive neuroendocrine tumors of the pancreatic origin (PNET) [23], and advanced estrogen receptor (ER) positive, human epidermal growth factor receptor-2 (HER2) negative breast cancer [24]. A phase 1 study of everolimus plus weekly cisplatin in combination with intensity-modulated radiation therapy in head and neck cancer has very recently been conducted [25]. However, this study mainly evaluated pharyngeal and salivary gland cancers, with only a few cases of oral cancer being included. As chemosensitivity is known to differ between pharyngeal cancer, salivary gland cancer, and oral cancer, a further examination of only oral cancer is needed.

In the present study, we selected patients who underwent radical surgery and examined the relationship between activated mTOR and clinical outcomes, and the antitumor activity of everolimus using OSCC cell lines.

Materials and Methods

Patients

Paraffin-embedded sections were obtained from the biopsy specimens of 70 patients with OSCC who underwent radical surgery in our Department between January 2000 and December 2007. The tumor stage was classified according to the TNM classification of the International Union Against Cancer [39]. The histological differentiation of tumors was defined according to the WHO classification [40]. The

pattern of invasion was classified according to Bryne's classification [41].

Immunohistochemical staining and evaluation

Deparaffinized sections in xylene were soaked in 10 mmol/l citrate buffer (pH 6.0) and placed in an autoclave at 121˚C for 5 min for antigen retrieval. Endogenous peroxidase was blocked by incubating sections with 0.3% H_2O_2 in methanol for 30 min. Immunohistochemical staining was performed using the Envision system (ENVISION+; DAKO, Glostrup, Denmark). The primary antibodies used were against phosphorylated mTOR (p-mTOR) and proliferating cell nuclear antigen (PCNA). The sections were then washed in Dulbecco's phosphate buffered saline (PBS), followed by incubation with the primary antibodies at 4˚C overnight. The reaction products were visualized by immersing the sections in diaminobenzidine (DAB) solution, and the samples were counterstained with Meyer's hematoxylin and mounted. Results were evaluated by calculating the total immunostaining score as the product of the proportional score and intensity score. As described previously, the proportional scores described the estimated fraction of positively-stained tumor cells (0, none; 1, <10%; 2, 10-50%; 3, 50- 80%; 4, >80%). The intensity score represented the estimated staining intensity (0, no staining; 1, weak; 2, moderate; 3, strong). Total scores ranged from 0-12. Positive sections were defined as those with a total score >4 [37]. Immunohistochemical overexpression was defined as a total score greater than 4 because immunohistochemical expression in samples showed a bimodal distribution with the discriminating nadir at a total score value of 3 to 4.

Reagents and cell culture

Everolimus was purchased from Selleck-chemicals (Houston, TX USA). It was dissolved in DMSO and adjusted to the final concentration with culture medium. All 7 human OSCC cell lines, SAS, HSC-2, HSC-3, HSC-4, OSC-20, SCC25, and Ca9-22,

used in this study were cultured in a 1:1 mixture of Ham's F-12/DMEM supplemented with 10% FBS (Trace Scientific, Melbourne, Australia). The cells were exposed to normoxia or hypoxia in the presence or absence of different doses of everolimus. All cells were maintained under humidified 5% CO_2 and 19% O_2 incubation at 37˚C (normoxic conditions). Hypoxic conditions (0.1% O_2) were achieved using AneroPack-Kenki (Mitsubishi Gas Chemical) and were monitored using an oxygen indicator.

Cell proliferation assay

Cells were seeded in 96-well plates at a concentration of 1.5×10^3 per well and incubated for 24h. Cells were exposed to everolimus doses ranging from 0.001nmol/L to 1000nmol/L. At the end of the treatment for 72h, cells were incubated with 0.5mg/ml 3-(4, 5-dimethylthiazol-2-yl)-2, 5-diphenyltetrazolium bromide (MTT; Sigma-Aldrich). Four hours later, the medium was replaced with 100μl dimethylsulfoxide (DMSO; Sigma-Aldrich) and vortexed for 10 min. Absorbance was then recorded at 570nm using a microplate auto reader (Multiskan FC, Thermo Fisher Scientific Inc). Cell viability (%) was calculated as a percentage of the absence of everolimus. The 50% of cell growth inhibition (IC_{50}) values were appropriately derived from the results obtained with the MTT assay.

Invasion assay

A Biocoat Matrigel invasion chamber containing an internal chamber with an 8-μm porous membrane bottom coated with Matrigel (Becton Dickinson, Bedford, MA) was used for the invasion assay. Six-well cell culture inserts and a six-well multiwall companion plate were used for the experiment. The membranes were rehydrated with warm serum-free medium for 2h. The internal chamber was filled with 1.25×10^5 cells in medium containing 10% FBS as a chemoattractant. Cells were incubated for 72h

under normoxic conditions, non-invading cells were removed from the top of the wells with a cotton swab, and cells that were transferred to the inverse surface of the membrane were subjected to Diff-Quick staining. Cells were counted under a microscope at 100 × magnification. Cells that passed through a control chamber without Matrigel were counted for the control. All experiments were performed in triplicate, and cell numbers were counted in at least 2 fields/well. The ratio of the cell count that passed through the Matrigel chamber to the control cell count was defined as the invasion index, and was expressed as a percentage.

Wound-healing assay

Cell migration was evaluated by a scratched wound-healing assay on plastic plate wells. In brief, cells were grown to confluency and then wounded using a pipette tip. Three wounds were made for each sample, and all were photographed at 0h and subsequent time points. Cell migration was evaluated by measuring the width of the wound at the same position.

Western blot analysis

Cells were harvested by trypsinization, washed, and precipitated by centrifugation. The Mammalian Cell Extraction Kit (Biovison Research Products, Mountain View, CA) was used to extract proteins. All subsequent manipulations were performed on ice. The cells were incubated in Extraction Buffer Mix. Lysed cells were centrifuged at 15000rpm for 5min, and the resultant supernatant was used. The protein concentration of each sample was measured with micro-BCA protein assay reagent (Pierce Chemica. Co., Rockford, IL). After the samples were denatured in SDS sample buffer, they were heated at 70 ˚C for 10mins and then loaded onto a 4-12% NuPAGE NOVEX bis-Tris polyacrylamide gel or 3-8% NuPAGE NOVEX Tris-Acetate polyacrylamide gel. After electrophoresis, the separated proteins were transferred to iBlot polyvinylidene

difluoride membranes using the iBlot Dry Blotting System and signals were detected by the Western Breeze Immunodetection Kit (life technologies, Tokyo, Japan). Antibodies against mTOR, p-mTOR, $p70^{S6K}$, $p\text{-}p70^{S6K}$, 4E-BP1, p-4E-BP1 (Cell Signaling Technology, Danvers, MA), HIF-1α (Abcam, Tokyo, Japan) and VEGF-C (life technologies, Tokyo, Japan) were used at 1:1000 dilution. Anti-β-actin (Santa Cruz Biotech, CA) was used as a blotting control.

Statistical analysis

The relationships between the sample expression of target molecules and clinicopathological features were assessed by Fischer's exact test. Continuous data were given as means ± standard deviation. Survival analysis was calculated using the Kaplan-Meier method and compared using the log-rank test. A multiple regression study was performed using Cox's proportional hazard analysis. Predictors that were not associated with the disease-specific survival (DSS) rate were not included in the multivariate analysis. Differences between groups were compared with the t-test. P values less than 0.05 were considered significant.

Results

Expression of p-mTOR in OSCC

p-mTOR protein expression was absent or minimal in the cytoplasm of epithelial cells in normal oral tissue. However, p-mTOR was overexpressed in 37 (52.8%) out of 70 OSCC samples. p-mTOR was mainly expressed in the cytoplasm of tumor cells, ranging from low to strong intensities. p-mTOR expression was observed in tumor nests and the invasive front, and was stronger in the invasive front (Fig. 1).

Relationship between p-mTOR expression and clinicopathological factors and survival.

p-mTOR expression levels in OSCC specimens were examined as a function of

clinicopathological factors. The expression of p-mTOR was correlated with the tumor stage and regional lymph node metastasis. However, no correlation was observed between oral cancer cell invasion and p-mTOR expression (Table 1).

The 5-year DSS rates were determined according to p-mTOR expression and other clinicopathological factors. Univariate analysis using the log-rank test and Kaplan-Meier method revealed a correlation between p-mTOR expression and 5-year DSS rates (Fig. 2, $P<0.05$). Predictors that were associated with 5-year DSS rates in univariate analysis were included in Cox's proportional hazard model, and this multivariate analysis showed that p-mTOR expression was not a significant independent predictor of 5-year DSS in OSCC (Table 2, $p=0.397$).

Relationship between mTOR activity and the PCNA labeling index

PCNA expression levels were immunohistochemically examined in cancer cells to determine the interaction between tumor cell proliferation and the function of mTOR. PCNA expression was detected immunohistochemically in the nuclei of tumor cells. The average PCNA labeling index (LI) was significantly higher in p-mTOR positive cases (51.595%) than in p-mTOR negative cases (23.379%) ($P<0.001$).

Inhibition of mTOR by everolimus suppressed cell growth in OSCC cell lines.

We evaluated the sensitivity of everolimus in the 7 different OSCC cell lines using the MTT assay. Everolimus significantly inhibited cell proliferation in a dose-dependent manner in all cell lines tested (Fig. 3A, $P<0.05$). SAS was the most sensitive cell line, followed by HSC-2 (IC_{50}, 3.65, 7.38nM, respectively). We selected the most sensitive cell line, SAS and analyzed the expression levels of the phosphorylated and non-phosphorylated forms of mTOR, $p70^{S6K}$, and 4E-BP1 by western blotting. The results obtained showed that the phosphorylation of p-mTOR, $p70^{S6K}$, and p-4E-BP1 was inhibited in a dose-dependent manner (Fig. 3B).

Effect of everolimus on the migration and invasion of SAS cells

Cell migration and invasion are the basic characteristics of tumor growth and metastasis. We performed wound healing and Matrigel invasion assays on SAS cells to examine the effects of everolimus on the migration and invasion potential of cells. The evaluation of cell migration in the control condition, 1nM of everolimus, 10nM of everolimus, and 100nM of everolimus revealed that healing rate at 12h after wounding was significantly decreased (Fig. 4A, $P<0.05$). The evaluation of invasion potential also revealed a significant decrease in the invasion index (Fig. 4B, $P<0.05$). These results indicated that everolimus suppressed the mobility of SAS cells *in vitro*.

Effect of everolimus under hypoxic conditions

We analyzed the effect of everolimus on the HIF-1 pathway to clarify the chemoresistance under hypoxic conditions. A comparison of the effects of the control condition, 1nM of everolimus, 10nM of everolimus, and 100nM of everolimus on the expression of HIF-1α and VEGF-C revealed a dose-dependent decrease in expression levels (Fig. 5). These results indicate that everolimus may be effective both normoxic and hypoxic conditions.

Discussion

The goal of this study was to assess the relationship between activated mTOR and clinical outcomes, and the antitumor activity of everolimus using OSCC cell lines. We here demonstrated that p-mTOR was overexpressed in 52.8% of OSCC. Monteiro et al. [13] reported the strong expression of p-mTOR in 63.9% of head and neck carcinomas, while Clark et al. [26] reported its expression in 81.9%, and Brown et al. [27] reported its expression in 93%. Hirashima et al. [14] also confirmed the expression of p-mTOR in 49.7% of esophageal squamous cell carcinoma. Our expression data are equal or lower than previously reported values. This may have been due to differences in the

anatomical locations of the tumors, methods used to evaluate mTOR phosphorylation, or cut-off values for p-mTOR positivity. Regarding the clinicopathological features and survival, the results of the present study are consistent with previous findings in which a close relationship was observed between elevated p-mTOR levels and poorer survival rates [13-16, 26, 27]. PCNA has been considered to be a potent cell proliferation maker and its clinical significance has been established in OSCC [28]. Our results suggest that mTOR expression levels could be a prognostic factor in OSCC patients.

In this context, we examined the antitumor activity of the mTOR inhibitor everolimus in OSCC cell lines under normoxic and hypoxic conditions. We showed here that mTOR inhibitor everolimus inhibited at the level of cell proliferation and protein expression of mTOR and its downstream signaling in a dose-dependent manner in OSCC. The discrepancy in IC_{50} values could be due to differences in the cell systems examined. Similar results have been reported for breast cancer, renal cell carcinoma, pancreatic neuroendocrine tumor, medullary thyroid carcinoma, gastric cancer, and ovarian clear cell adenocarcinoma [17, 32-36]. These findings suggest that everolimus as a single agent may have potent anti-tumor efficacy against OSCC cells.

Tumor invasion and metastasis in various cancers including OSCC are known to be regulated by various genetic instabilities [6, 7]. Previous studies demonstrated that the *de novo* overexpression of mTOR and downstream factors increased the invasion and migration potentials, whereas the inhibition of mTOR signaling by mTOR inhibitors decreased the invasion and migration potentials of esophageal squamous cell carcinoma [7, 32]. The immunohistochemical staining of p-mTOR in the present study revealed strong positivity in the invasive front of tumors. However, p-mTOR expression was not significantly correlated with an invasion pattern; therefore, we examined invasion and migration potentials in OSCC cell lines. We showed that everolimus inhibited invasion

and migration potentials in a dose-dependent manner, which was consistent with the findings of a recent study.

HIF-1α is significantly activated by hypoxia, and transactivates many genes, including VEGF, involved in tumor development [6, 7]. Recent studies reported that HIF-1α may be involved in chemoradioresistance. Moreover, the HIF-1α/VEGF pathway has been correlated with highly aggressive disease and poor prognosis in some cancers [29-31, 36]. We also previously demonstrated that the mTOR/HIF-1α/VEGF pathway was associated with clinical outcomes [37]. VEGF-C was shown to induce lymphangiogenesis and the formation of lymph node metastasis [29, 38]. We showed here that everolimus inhibited the expression of HIF-1α and VEGF-C under both normoxic and hypoxic conditions in a dose-dependent manner. Indeed, HIF-1α was efficaciously inhibited under hypoxic condition. These results indicated that the knockdown of HIF-1α expression may elevate sensitivity to various drugs under both normoxic and hypoxic conditions, and that everolimus could be useful for inhibiting tumor progression and metastasis.

In summary, mTOR activation was observed in half of the OSCC tumors examined, which suggested that mTOR could be a promising target for the anti-tumor effect of everolimus under both normoxic and hypoxic conditions. Although further experimental studies are needed to confirm these results, the results of the current study suggest a potential treatment strategy for OSCC patients.

Conflicts of interest statement

None declared.

Acknowledgements

This study was partially supported by Grants 70549609 from the Ministry of Education, Culture, Sports, Science and Technology, Japan.

References

1. Mao L, Hong WK and Papadimitrakopoulou VA (2004) Focus on head and neck cancer. Cancer Cell 5:311-6
2. Seiwert TY and Cohen EE (2005) State-of-the-art management of locally advanced head and neck cancer. Br J Cancer 92 (8):1341-8
3. Rogers SN, Brown JS, Woolgar JA, Lowe D, Magennis P, Shaw RJ, Sutton D, Errington D, Vaughan D (2009) Survival following primary surgery for oral cancer. Oral Oncol 45 (3):201-11
4. Shaw RJ, Cantley LC (2006) Ras, PI(3)K and mTOR signaling controls tumor cell growth. Nature 441 (7092):424-30
5. Liu FY, Zhao ZJ, Li P, Ding X, Zong ZH, Sun CF (2010) Mammalian target of rapamycin (mTOR) is involved in the survival of cells mediated by chemokine receptor 7 through PI3K/Akt in metastatic squamous cell carcinoma of the head and neck. Br J Oral Maxillofac Surg 48:291-6
6. Semenza GL. Targeting HIF-1 for cancer therapy. Nat Rev Cancer. Nat Rev Cancer 2003;3:721-32
7. Laplante M, Sabatini DM (2012) mTOR signaling in growth control and disease. Cell 149 (2):274-93
8. Pouysségur J, Dayan F, Mazure NM (2006) Hypoxia signaling in cancer and approaches to enforce tumour regression. Nature 441:437-43
9. Hohwer N, Cramer T (2011) Hypoxia-mediated drug resistance: Novel insights on the functional interaction of HIFs and cell death pathways. Drug Resist Updat

14:191-201

10. Brown LM, Cowen RL, Debray C, Eustace A, Erier JT, Sheppard FC, Parker CA, Stratford IJ, Williams KJ (2006) Reversing hypoxic cell chemoresistance in vitro using genetic and small molecule approaches targeting hypoxia inducible factor-1. Mol Pharmacol 69:411-8
11. Liu L, Ning X, Sun L, Zhang H, Shi Y, Guo C, Han Z, Liu J, Sun S, Han Z, Wu K, Fan D (2008) Hypoxia-inducible factor-1 alpha contributes to hypoxia-induced chemoresistance in gastric cancer. Cancer sci 99:121-8
12. Yoshiba S, Ito D, Nagumo T, Shirota T, Hatori M, Shintani S (2009) Hypoxia induces resistance to 5-fluorouracil in oral cancer cells via G(1) phase cell cycle arrest. Oral Oncol 45:109-15
13. Monteiro LS, Delgado ML, Ricardo S, Garcez F, do Amarai B, Warnakulasuriya S, Lopes C (2013) Phosphorylated mammalian target of rapamycin is associated with an adverse outcome in oral squamous cell carcinoma. Oral Surg Oral Med Oral Pathol Oral Radiol 115(5):638-45
14. Hirashima K, Baba Y, Watanabe M, Karashima R, Sato N, Imamura Y Hiyoshi Y, Nagai Y, Hayashi N, Iyama K, Baba H (2010) Phosphorylated mTOR expression is associated with poor prognosis for patients with esophageal squamous cell carcinoma. Ann Surg Oncol 17(9):2486-93
15. Bakarakos P, Theohari I, Nomikos A, Mylona E, Papadimitriou C, Dimopoulos AM, Nakopoulou L (2010) Immunohistochemical study of PTEN and phosphorylated mTOR proteins in familial and sporadic invasive breast carcinomas. Histopathology 56(7):876-82
16. Xu DZ, Geng QR, Tian Y, Cai MY, Fang XJ, Zhan YQ, Zhou ZW, Li W, Chen YB, Sun XW, Guan YX, Li YF, Lin TY (2010) Activated mammalian target of

rapamycin is a potential therapeutic target in gastric cancer. BMC Cancer 10:536

17. Del Bufalo D, Ciuffreda L, Trisciuoqlio D, Desideri M, Coqnetti F, Zupi G, Milella M (2006) Antiangiogenic potential of the Mammalian target of rapamycin inhibitor temsirolimus. Cancer Res 66:5549-54

18. Matsumoto K, Arao T, Tanaka K, Kaneda H, Kudo K, Fujita Y, Tamura D, Aomatsu K, Tamura T, Yamada Y, Saijo N, Nishio K (2009) mTOR signal and hypoxia-inducible factor-1 alpha regulate CD133 expression in cancer cells. Cancer Res 69:7160-4

19. Okui T, Shimo T, Fukazawa T, Kurio N, Hassan NM, Honami T, Takaoka M, Naomoto Y, Sasaki A (2010) Antitumor effect of temsirolimus against oral squamous cell carcinoma associated with bone destruction. Mol Cancer Ther 9:2960-9

20. Okui T, Shimo T, Fukazawa T, Mohammad Monsur Hassan N, Honami T, Ibaragi S, Takaoka M, Naomoto Y, Sasaki A (2013) Novel HSP90 inhibitor NVP-AUY922 enhances the anti-tumor effect of temsirolimus against oral squamous cell carcinoma. Curr Cancer Drug Targets 13:289-99.

21. Huang S, Houghton PJ (2003) Targeting mTOR signaling for cancer therapy. Curr Opin Pharmacol 3:371-7

22. Motzer RJ, Escudier B, Oudard S, Hutson TE, Porta C, Bracarda S, Grunwald V, Thompson JA, Figlin RA, Hollaender N, Urbanowitz G, Berg WJ, Kay A, Lebwohl D, Ravaud A; RECORD-1 Study Group (2008) Efficacy of everolimus in advanced renal cell carcinoma: a double-blind, randomized, placebo-controlled phase III trial. Lancet 372:449-56

23. Pavel ME, Hainsworth JD, Baudin E, Peeters M, Hörsch D, Winkler RE, Klimovsky J, Lebwohl D, Jehl V, Wolin EM, Oberg K, Van Cutsem E, Yao JC; RADIANT-2

Study Group (2011) Everolimus plus octreotide long-acting repeatable for the treatment of advanced neuroendocrine tumours associated with carcinoid syndrome (RADIANT-2): a randomised, placebo-controlled, phase 3 study. Lancet 378:2005-12

24. Burris HA 3rd, Lebrun F, Rugo HS, Beck JT, Piccart M, Neven P, Baselga J, Petrakova K, Hortobagyi GN, Komorowski A, Chouinard E, Young R, Gnant M, Pritchard KI, Bennett L, Ricci JF, Bauly H, Taran T, Sahmoud T, Noguchi S (2013) Health-related Quality of Life of Patients with Advanced Breast cancer Treated With Everolimus Plus Exmestane Versus Placebo Plus Exemestane in the Phase 3, Randomizd, Controlled, BOLERO-2 Trial. Cancer 119(10):1908-15
25. Fury MG, Lee NY, Sherman E, Ho AL, Rao S, Heguy A, Shen R, Korte S, Lisa D, Ganly I, Patel S, Wong RJ, Shaha A, shah J, Haque S, Katabi N, Pfister DG (2013) A phase 1 study of everolimus + weekly cisplatin + intensity modulated radiation therapy in head and neck cancer. Int J Radiat Oncol Biol Phys 87(3):479-86
26. Clark C, Shah S, Herman-Ferdinandez L, Ekshyyan O, Abreo F, Rong X, McLarty J, Lurie A, Milligan EJ, Nathan CO (2010) Teasing out the best molecular marker in the AKT/mTOR pathway in head and neck squamous cell cancer patients. Laryngoscope 20(6):1159-65
27. Brown RE, Zhang PL, Lun M, Zhu S, Pellitteri PK, Riefkohl W, Law A, Wood GC, Kennedy TL (2006) Morphoproteomic and pharmacoproteomic rationale for mTOR effectors as therapeutic targets in head and neck squamous cell carcinoma. Ann Clin Lab Sci 36(3):273-82
28. Myoung H, Kim MJ, Lee JH, Ok YJ, Paeng JY and Yuun PY (2006) Correlation of proliferative markers (Ki-67 and PCNA) with survival and lymph node metastasis in oral squamous cell carcinoma: a clinical and histopathological analysis of 113

patients. Int J Oral Maxillofac Surg 35(11):1005-10

29. Dorević G, Matusan-Ilijas K, Babarović E, Hadzisejdić I, Grahovac M, Grahovac B, Jonjic N (2009) Hypoxia inducible factor-1alpha correlates with vascular endothelial growth factor A and C indicating worse prognosis in clear cell renal cell carcinoma. J Exp Clin Cancer Res 20; 28-40
30. Cao D, Hou M, Guan YS, Jiang M, Yang Y, Gou HF (2009) Expression of HIF-1alpha and VEGF in colorectal cancer: association with clinical outcomes and prognostic implications. BMC Cancer 9:432
31. Oh SY, Kwon HC, Kim SH, Jang JS, Kim MC, Kim KH, Han JY, Kim CO, Kim SJ, Jeong JS, Kim HJ (2008) Clinicopathologic significance of HIF-1alpha, p53, and VEGF expression and preoperative serum VEGF level in gastric cancer. BMC Cancer 8:123
32. Juengel E, Engler J, Natsheh I, Jones J, Mickuckyte A, Hudak L, Jonas D, Blaheta RA (2009) Combining the receptor tyrosine kinase inhibitor AEE788 and the mammalian target of rapamycin (mTOR) inhibitor RAD001 strongly inhibits adhesion and growth of renal cell carcinoma cells. BMC Cancer 9:161
33. Zitzmann K, De Toni EN, Brand S, Göke B, Meinecke J, Spöttl G, Meyer HH, Auernhammer CJ (2007) The novel mTOR inhibitor RAD001 (everolimus) induces antiproliferative effects in human pancreatic neuroendocrine tumor cells. Neuroendocrinology 85(1):54-60
34. Grozinsky-Glasberg S, Rubinfeld H, Nordenberg Y, Gorshtein A, Praiss M, Kendler E, Feinmesser R, Grossman AB, Shimon I (2010) The rapamycin-derivative RAD001 (everolimus) inhibits cell viability and interacts with the Akt-mTOR-p70S6K pathway in human medullary thyroid carcinoma cells. Mol Cell Endocrinol 315:87-94

35. Nishi T, Iwasaki K, Ohashi N, Tanaka C, Kobayashi D, Nakayama G, Koike M, Fujiwara M, Kobayashi T, Kodera Y (2013) Phosphorylation of 4E-BP1 predicts sensitivity to everolimus in gastric cancer cells. Cancer Lett 331(2):220-9
36. Miyazawa M, Yasuda M, Fujita M, Kajiwara H, Hirabayashi K, Takekoshi S, Hirasawa T, Murakami M, Ogane N, Kiguchi K, Ishiwata I, Mikami M, Osamura RY (2009) Therapeutic strategy targeting the mTOR-HIF-1alpha-VEGF pathway in ovarian clear cell adenocarcinoma. Pathol Int 59:19-27
37. Naruse T, Kawasaki G, Yanamoto S, Mizuno A and Umeda M (2011) Immunohistochemical study of VEGF expression in oral squamous cell carcinomas: correlation with the mTOR- HIF-1α pathway. Anticancer Res (12):4429-37.
38. Otrock ZK, Makarem JA and Shamseddine AI (2007) Vascular endothelial growth factor family of ligands and receptors: review. Blood Cells Mol Dis 38(3):258-68
39. Sobin LH, Wittekind C (2002) UICC TNM classification of malignant tumours, 6th edn. Wiley, New York
40. Pinborg JJ, Reichart PA, Smith CJ, van der Waal I (eds) (1997) World Health Organization histological typing of cancer and precancer of the oral mucosa, 2nd edn. Springer, New York
41. Bryne M, Boysen M, Alfsen CG, Abeler VM, Nesland JM, Kristensen GB, Piffko J, Bankfalvi A (1998) The invasive front of carcinomas. The most important area for tumour prognosis? Anticancer Res 18(6B):4757-64

Figure legends

Figure 1. Representative immunohistochemical staining for p-mTOR. Negative staining of p-mTOR is shown in the normal oral epithelium (A). Moderate p-mTOR cytoplasmic expression (staining index of 8) was observed in squamous cell carcinoma

with a Bryne's score of 2 (B). Strong p-mTOR cytoplasmic expression (staining index of 12) was observed in squamous cell carcinoma with a Bryne's score of 3 (C).

Figure 2. Kaplan-Meier survival curve of 5-year disease-specific survival (DSS) rates. The 5-year DSS rates of p-mTOR positive patients were significantly shorter than those of p-mTOR negative patients ($P<0.05$).

Figure 3. Effect of everolimus on cell proliferation and mTOR signaling in OSCC cell lines. Seven OSCC cell lines were exposed to doses of everolimus ranging from 0.001nM to 1000nM. The percentage cell viability (%) and dose of the drug that inhibited cell growth by 50% (IC_{50}) were calculated (A). SAS cells were exposed to everolimus at the indicated concentrations and subsequently assessed for protein expression and phosphorylation by western blotting (B).

Figure 4. Effect of everolimus on invasion and migration potentials in the SAS cell line. Invasion in SAS cells (left) and the percentage of invaded cells (right) were determined, as described in the Materials and Methods (A). The graph shows a significant decrease in the invasion index of SAS cells (58.87%, 35.28%, 19.06%, and 16.68%, respectively. $p<0.05$). The wound healing process was photographed 0, 3, 6, and 12 h after wounding (left), and healing rates were determined, as described in the Materials and Methods (B). The graph shows a significant decrease in the wound healing rate in SAS cells (83.33%, 68%, 51.84%, and 44.09%, respectively. $p<0.05$).

Figure 5. Effect of everolimus on the expression of HIF-1α and VEGF-C in the SAS cell line. Western blot analysis of HIF-1α and VEGF-C protein expression in SAS cells

exposed to normoxic and hypoxic conditions for 24h in the presence or absence of everolimus at the indicated concentrations.

Table 1. Relationship between the overexpression of p-mTOR and clinicopathological features and survival.

Table 2. Multivariate analysis (Cox regression) of DSS rates in OSCC.

Fig 1. Representative immunohistochemical staining for p-mTOR.

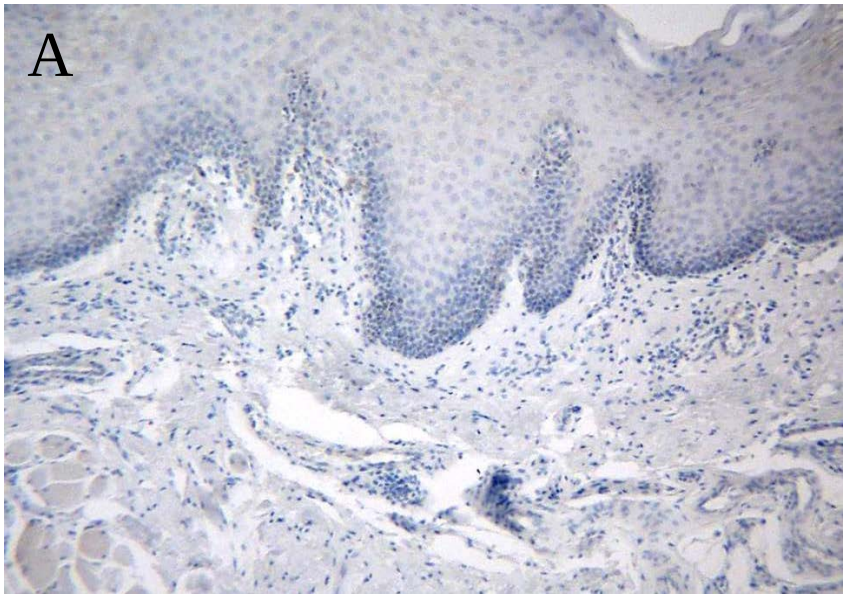

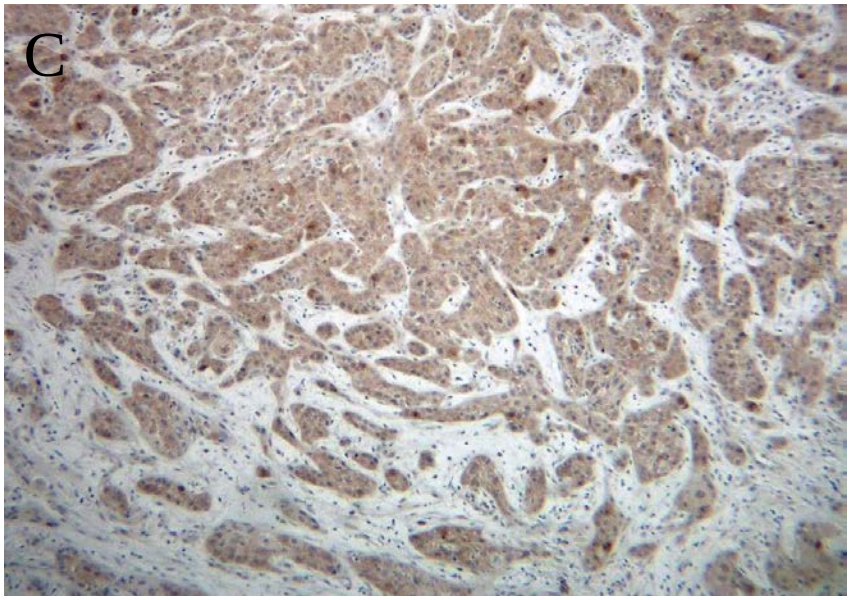

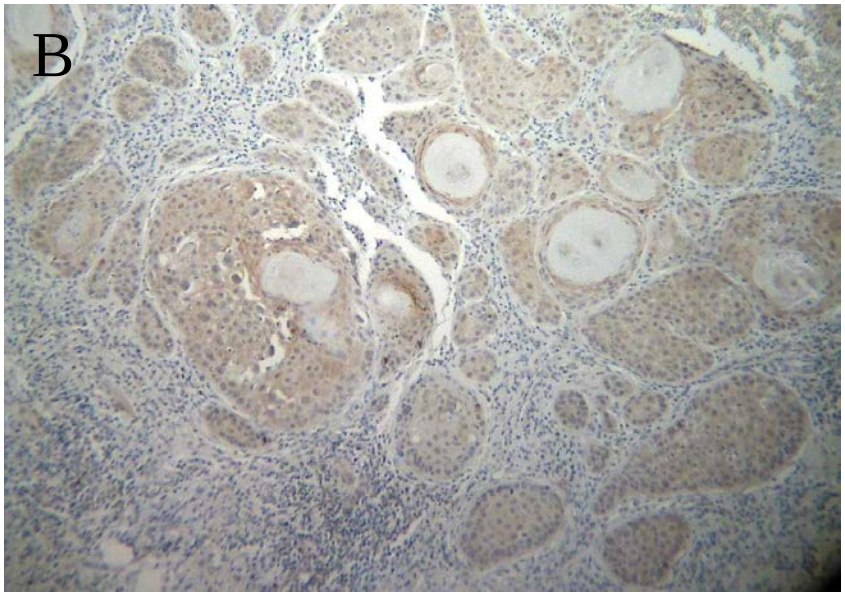

Fig 2. Kaplan-Meier survival curve of the 5-year disease-specific survival (DSS) rates.

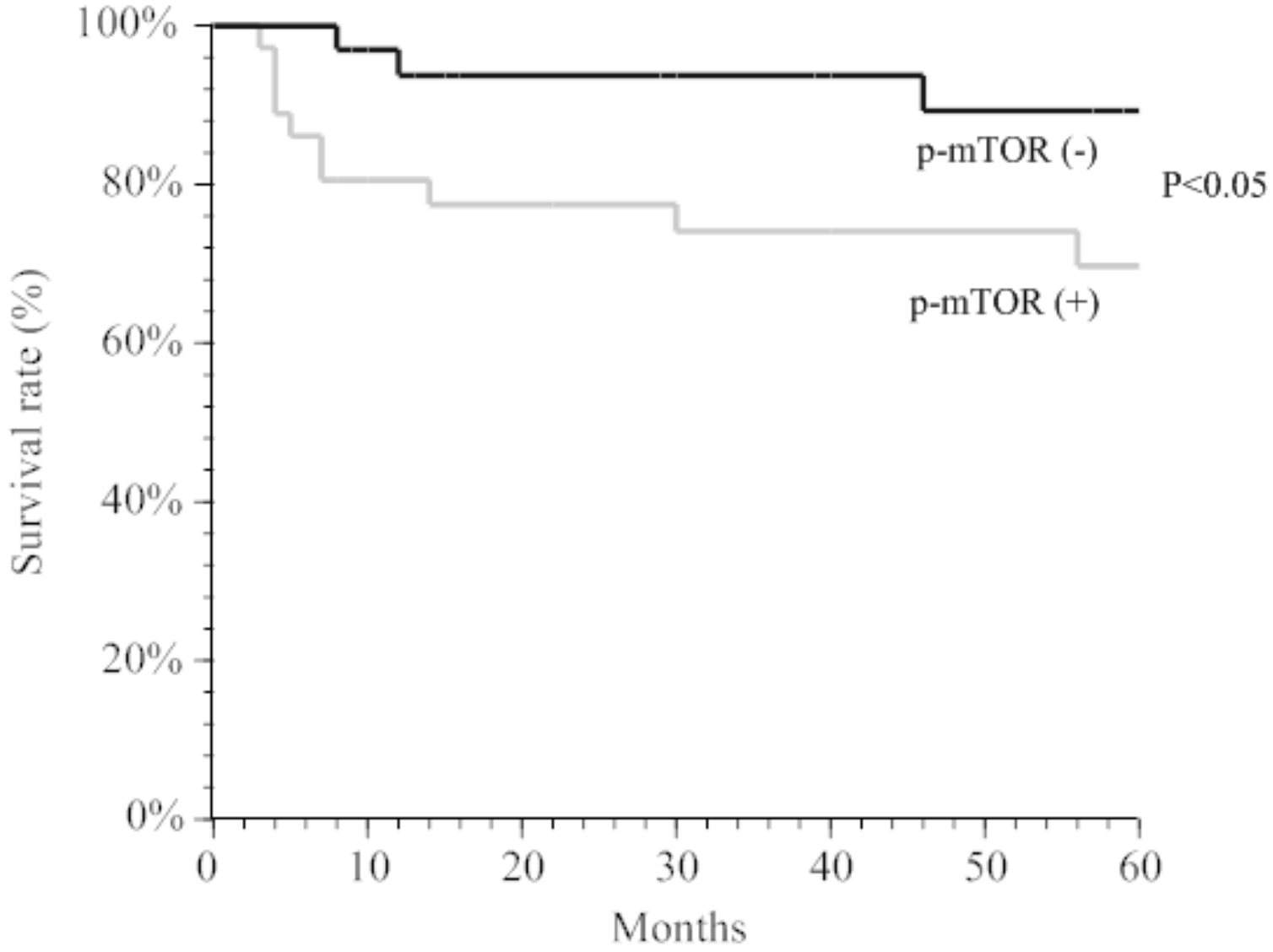

Fig 3. Effect of everolimus on cell proliferation and mTOR singanling in OSCC cell lines.

A

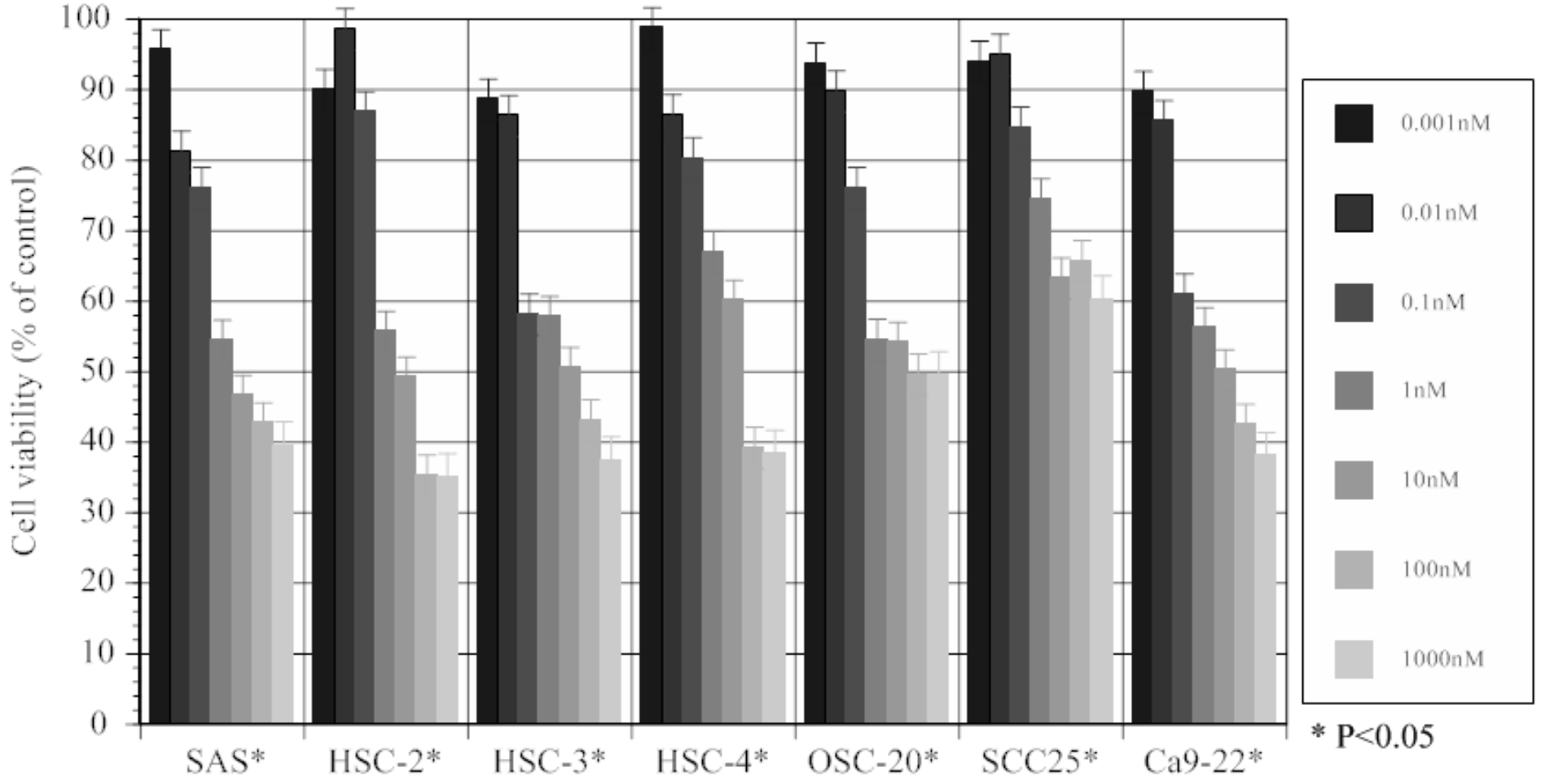

	SAS*	HSC-2*	HSC-3*	HSC-4*	OSC-20*	SCC25*	Ca9-22*
IC_{50} (nM)	3.65	7.38	11.8	30.35	81.27	1000	10.56

Fig 3. Effect of everolimus on cell proliferation and mTOR singanling in OSCC cell lines.

B

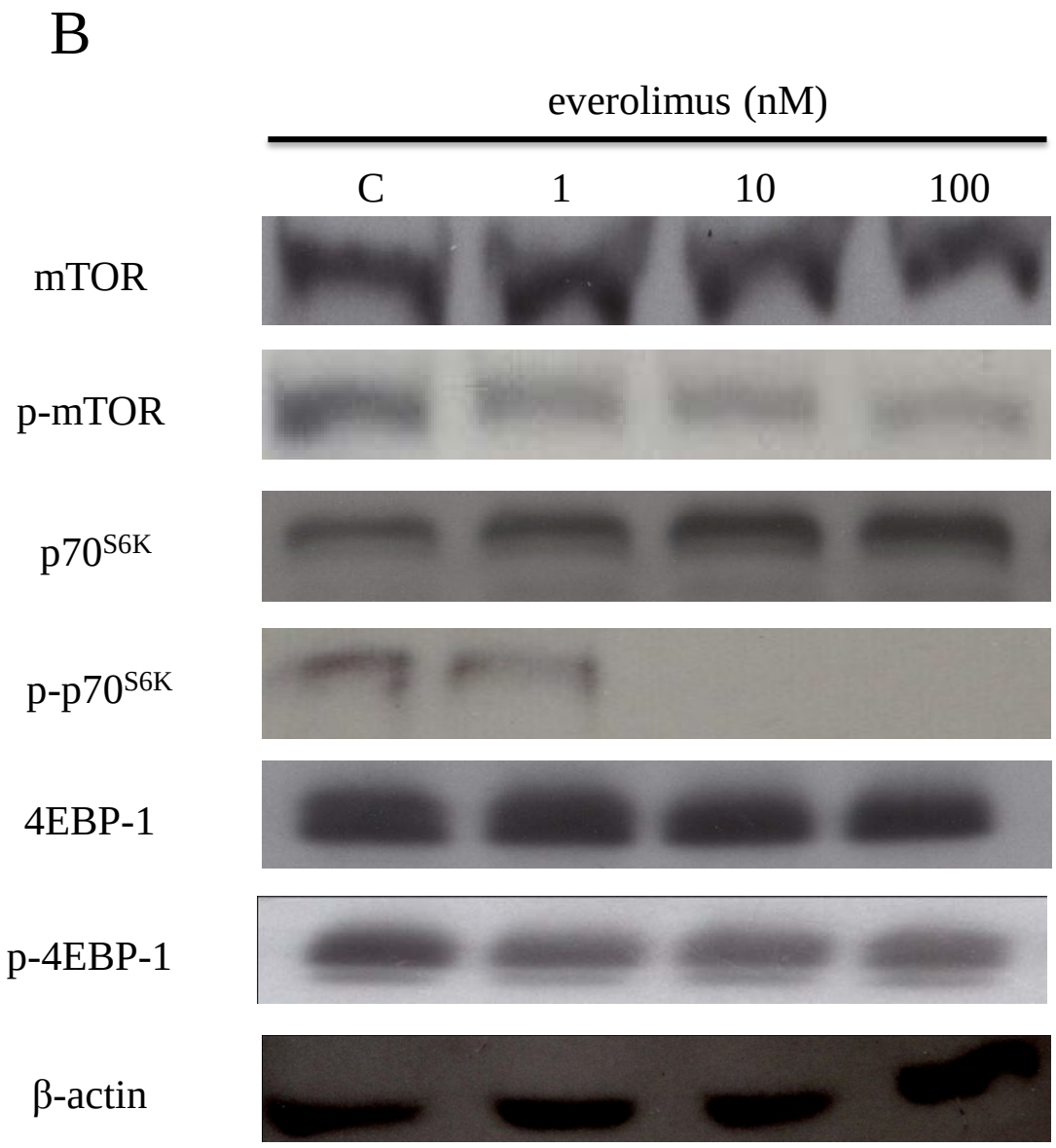

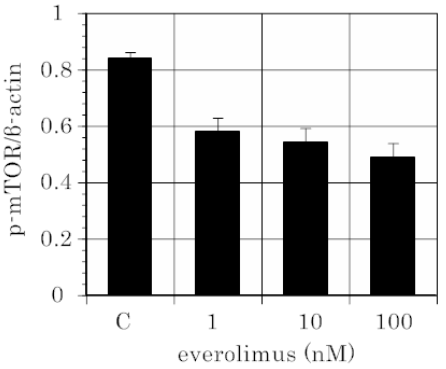

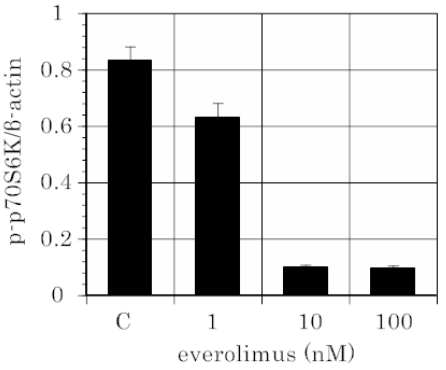

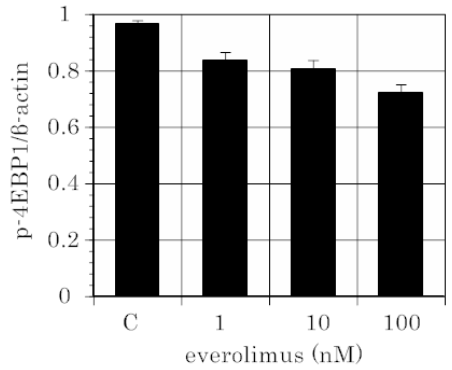

Fig 4. Effect of everolimus on invasion and migration potential in SAS cell line.

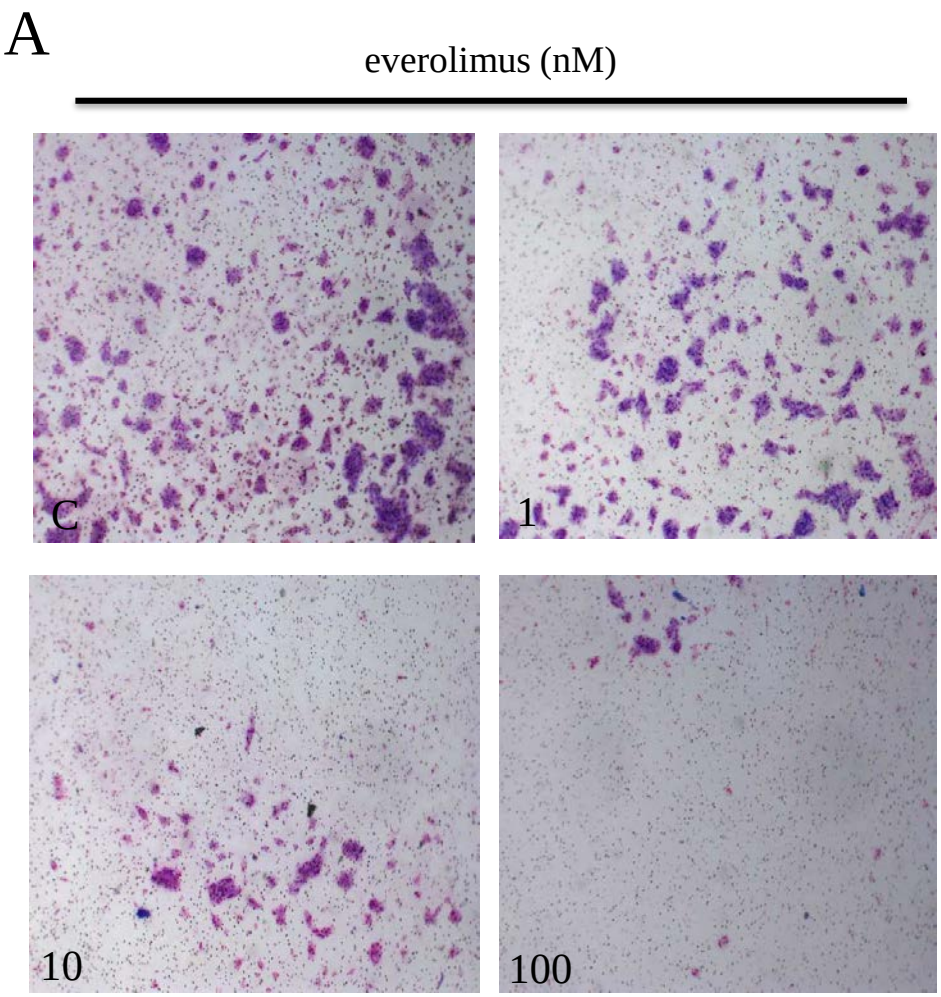

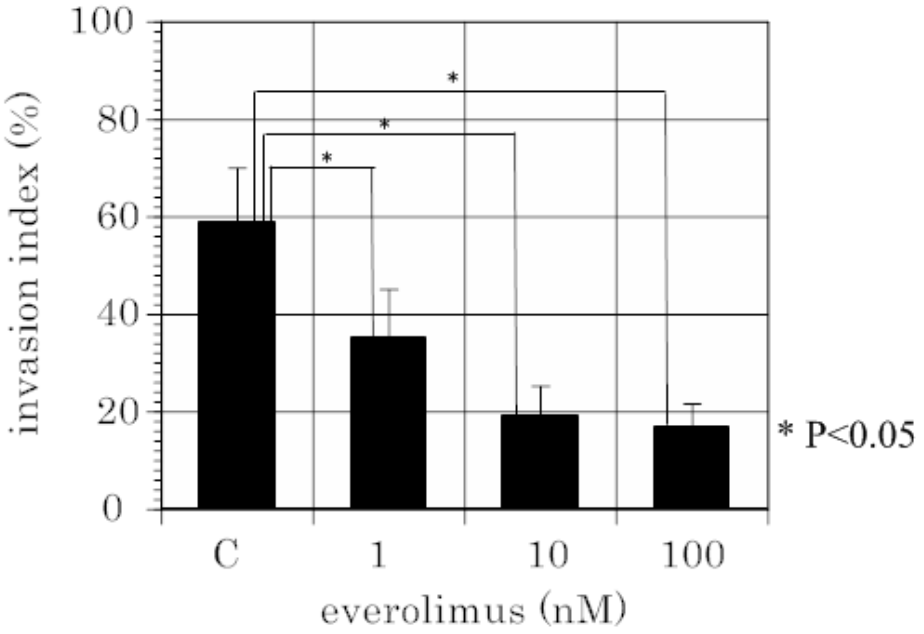

Fig 4. Effect of everolimus on invasion and migration potential in SAS cell line.

B

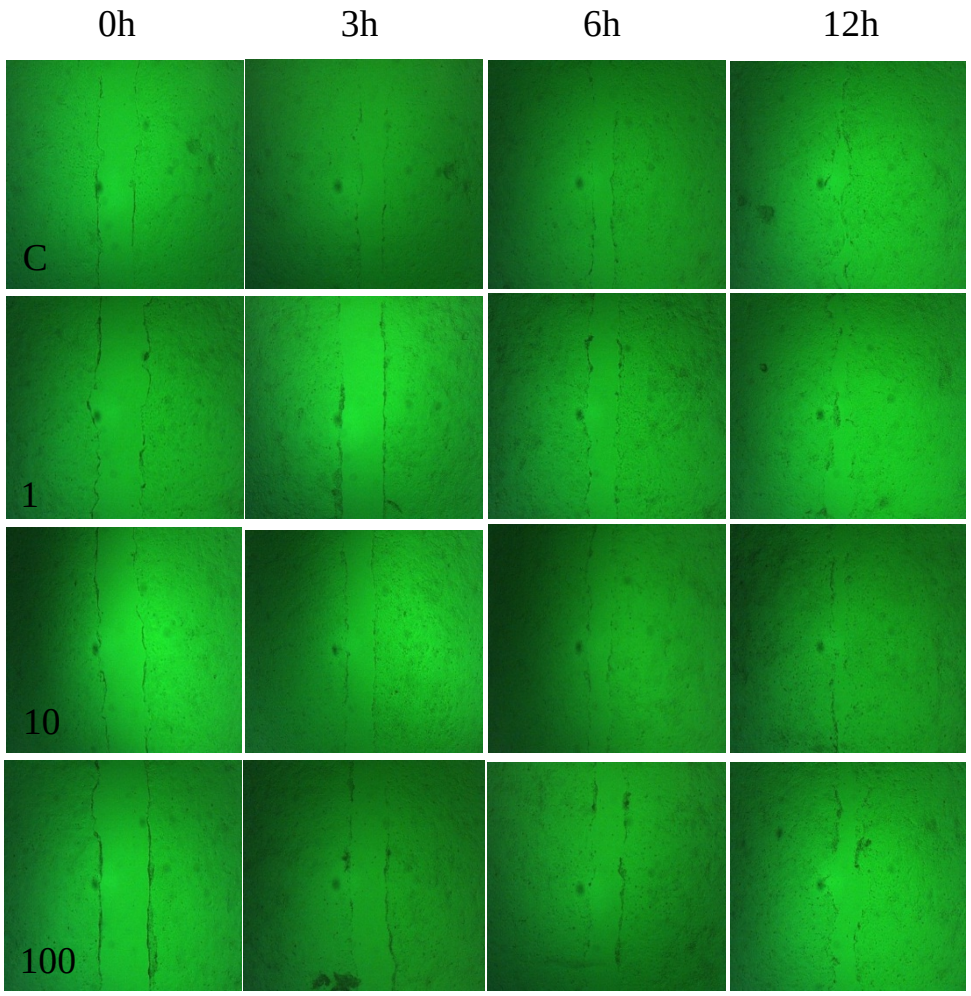

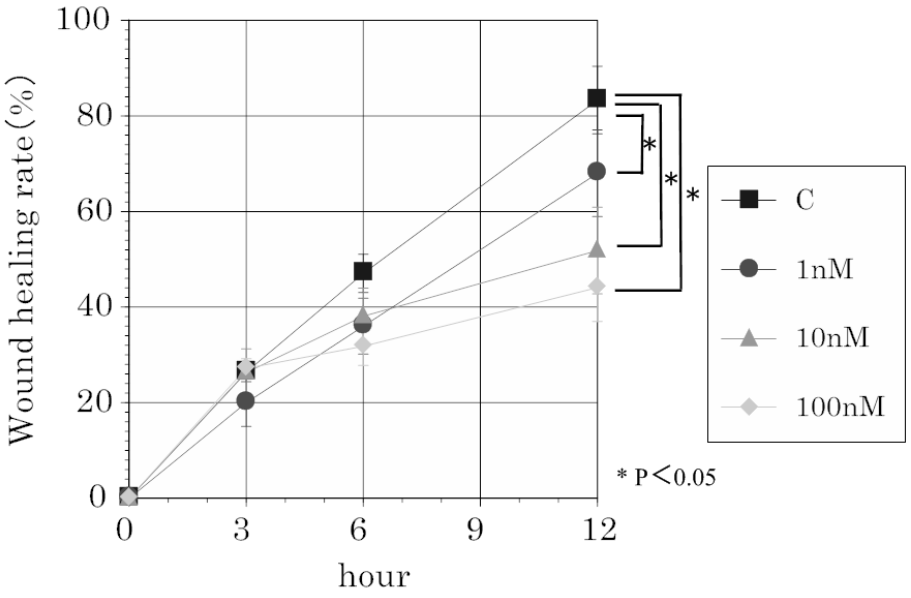

Fig 5. Effects of everolimus on HIF-1α and VEGF-C expressions in SAS cell line.

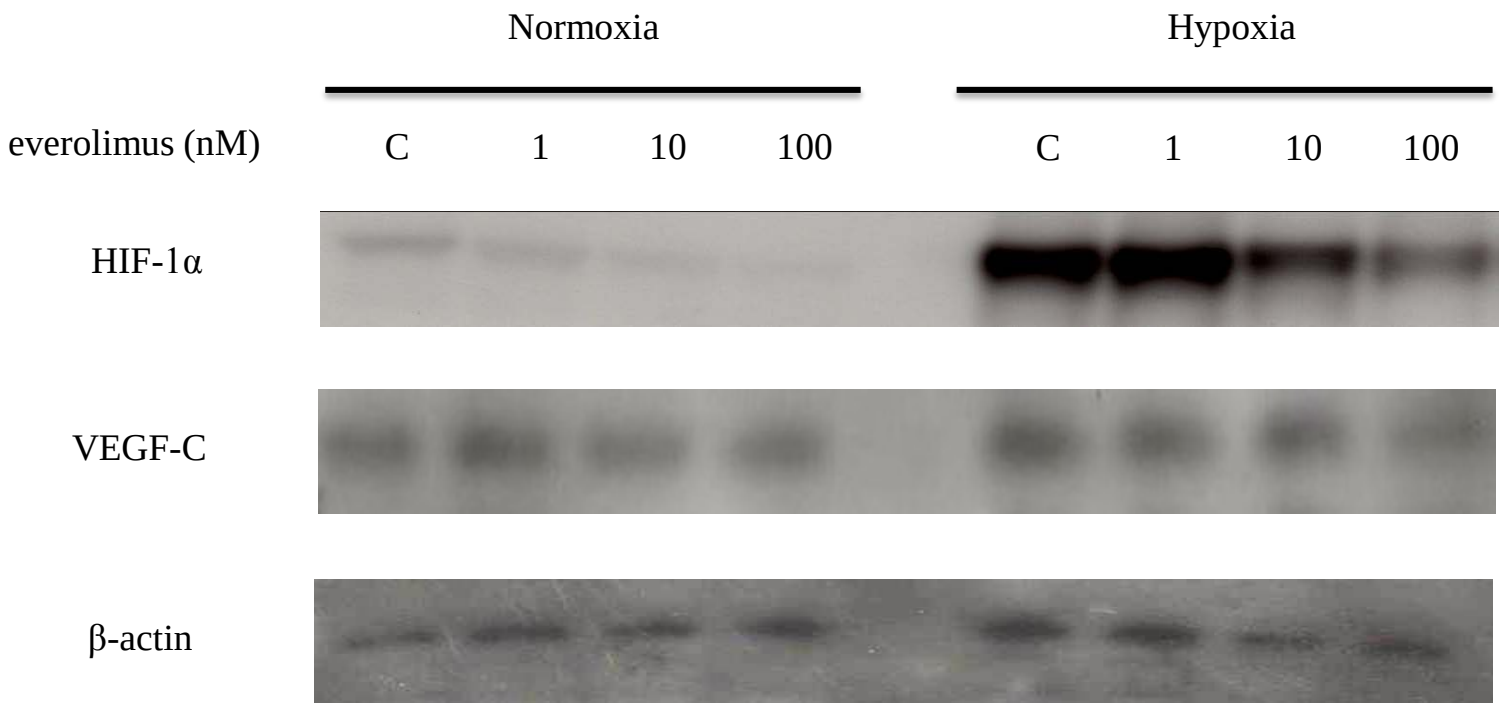

Table 1: Relationship between the overexpression of p-mTOR and clinicopathological features and survival.

		p-mTOR		*P*-value	5-year DSS (%)	*P*-value
		−	+			
Normal epithelium		10	0	<0.001		
SCC		33	37			
Gender	Male	21	20	0.472	73.7%	0.301
	Female	12	17		82.7%	
Age	67≧	11	15	0.623	83.5%	0.439
	67＜	22	22		76.2%	
T classification	T1+T2	29	22	<0.05	86.2%	0.02
	T3+T4	4	15		60.9%	
N classification	N0	30	25	<0.05	87.3%	<0.001
	N1+N2	3	12		48.6%	
Differentiation	well	31	33	0.676	80.8%	0.303
	moderate. poor.	2	4		66.7%	
Pattern of invasion	Grades 1/2	26	24	0.289	89.6%	<0.001
	Grades 3/4	7	13		52.9%	

Table 2: Multivariate analysis (Cox regression) of DSS rates in OSCC.

Parameter	Hazard ratio	95% CI	*P* value
T classification (T1 +T2 versus T3 + T4)	1.6271	0.4464-5.93	0.461
N classification (N0 versus N1 + N2)	2.7115	0.6774-10.85	0.158
Pattern of invasion (Grades 1/2 versus Grades 3/4)	6.7596	1.9943-22.91	0.002
p-mTOR overexpression (negative versus positive)	1.9025	0.43-8.42	0.397